Tellus (1986), *38B*, 250–261

An investigation by analytical transmission electron microscopy of individual insoluble microparticles from Antarctic (Dome C) ice core samples

By A. GAUDICHET[1,3], J. R. PETIT[2], R. LEFEVRE[1] and C. LORIUS[2], [1]*Laboratoire de Microscopie Analytique Appliquée aux Sciences de la Terre, Université Paris XII, Avenue Général de Gaulle—94010 Créteil Cedex, France;* [2]*Laboratoire de Glaciologie et Géophysique de l'Environnement, BP 96—38402 Saint-Martin d'Hères Cedex, France;* [3]*Laboratoire d'Etude des Particules Inhalées, 44, rue Charles Moureu—75013 Paris, France*

(Manuscript received September 16; in final form December 13, 1985)

ABSTRACT

Analytical transmission electron microscopy was used to study 225 insoluble microparticles in 6 ice samples formed under different climatic conditions over the last 30,000 years in the Antarctic Dome C ice core. The aim was to identify the mineralogy of dust and investigate the geographic location of sources and their variations with time.

As already suggested by previous work, it is confirmed that microparticles have mostly a terrigenous (aeolian) origin as revealed by identification of various clays (mostly illites), quartz and felspars in the 6 levels. Except for some products attributed to volcanic activity, the mineralogy of particles appears to be randomly mixed and shows no significant change nor particular signature of a specific source over the studied period. However, kaolinite, considered to be a tracer of low latitude dust source areas, was too low in content to suggest that the tropical area was a main source of Dome C dust over the studied period.

1. Introduction

Studies of ice samples from deep drillings in ice caps give information on the past climate and on the past aerosol content over time periods of many thousands of years (Dansgaard et al., 1971; Lorius et al., 1984; Wolff and Peel, 1985). Because mainly covered by ice (2 km thick ice cover) and far from aerosol dust sources, the central parts of the Antarctic continent, at elevation exceeding 3000 m above sea level, are generally considered as good observation grounds for the global aerosol background (Bigg, 1980; Shaw, 1980; Cunningham and Zoller, 1981). This is true for aerosol recorded in snow precipitation assuming a linear relationship between air and snow concentrations (Pourchet et al., 1983).

The 905 m Dome C (Fig. 1) deep drilling (74°S, 124°E, 3200 m elevation) has previously been studied for stable isotope and insoluble microparticle contents among other parameters. These components show large variations over the 30,000 year time period of this ice record (Fig. 2). Based on isotope contents (Lorius et al., 1979, 1984), climatic conditions over the last 10,000 years (or Holocene) have been similar to the present warm climate (called stage 1 on Fig. 2) with high values of $\delta^{18}O$ content, and were preceded, before a short transition (stage 2), by a very cold period (stage 3 and 4) extending from 15,000 BP to 30,000 BP. Stage 3 (15,000 BP to 25,000 BP) is thought to correspond to the Last Glacial Maximum (LGM).

Petit et al. (1981) and Briat et al. (1982) showed that the main portion of insoluble microparticles has a terrigeneous origin and represents the small-sized dust produced on the continents. Deserts and arid areas from the Southern Hemisphere are the potential sources of Antarctic microparticles. These authors found that during

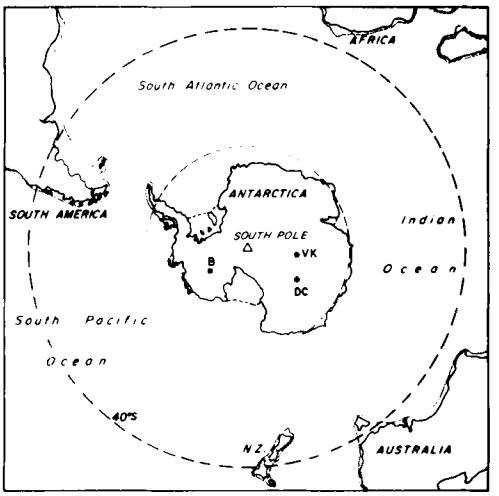

Fig. 1. Map of Southern hemisphere with 150 m-bathymetric contours and location of deep ice core drillings in Antarctica (B: Byrd; DC: Dome C; VK: Vostok).

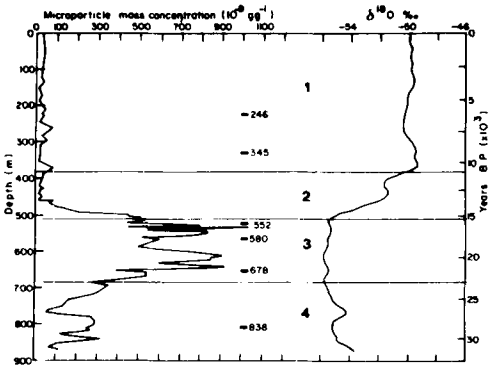

Fig. 2. Microparticle mass concentration and oxygen isotope ($\delta^{18}O‰$) variations along the Dome C ice core, adapted from Lorius et al. (1984). Isotope stage 1 to 4 and the positions of selected samples are indicated.

the LGM, there was an increase in the dust concentration by a factor about 15, compared to Holocene values, a trend which has also been observed on other ice cores from Antarctica and Greenland (Thompson, 1977; Cragin et al., 1977; Fisher 1979; Thompson and Mosley-Thompson, 1981; De Angelis et al., 1984). This was attributed to the large extension of global tropical aridity during the LGM as revealed by considerable geomorphological evidence from the continents (e.g. Sarnthein, 1978) and deep-sea sediments (Climap, 1976), coupled with a higher efficiency of atmospheric circulation for dust production and transport.

Low global volcanic activity over the last 30,000 years was also suggested, this because low level of volcanic tracers such as acid content, sulfate, zinc . . . The observations of many visible ash layers in the Byrd ice core (Gow and Williamson, 1971) and the discovery of glass shards in the Dome C core (Kyle et al., 1981), likely represent only the print of Antarctic volcanos now inactive. However, geographic location of the major dust sources of Antarctic microparticles remains unknown. Their identification through the study of specific source area tracers is of interest in tracking air masses over the Southern Hemisphere and also in estimating their respective contributions to atmospheric aerosol because dust may have an important impact on climate by modifying the radiative budget of the atmosphere. From the 907 m Dome C ice core, 6 samples were taken: 1 at level 838 m (stage 4) before the LGM period, 3 at levels 678 m, 580 m and 552 m covering the LGM (stage 3) period and 2 at levels 345 m and 246 m (stage 1) corresponding to the Holocene period (Fig. 2). This paper presents the results of the mineralogical identification of microparticles in Dome C samples, using Analytical Transmission Electron Microscopy (ATEM).

2. Analytical methods

The very low microparticle concentrations in Antarctica samples ($\simeq 20$ ng g^{-1} for Holocene samples) require clean sample processing conditions (class 100 dust free laboratory). The ice samples were 10 cm diameter, 15 cm long cylinders and represent 3 to 5 years of snow accumulation. To remove field contamination, we recored by melting the center of the ice with a thermal probe. The meltwater was divided in 15 ml aliquots. Aliquots were filtered through a Nuclepore membrane filter of 0.45 micron pore size and 13 mm in diameter, previously coated with a carbon layer. The volumes filtered, in the range of 5 to 50 ml, were chosen according to the microparticle concentrations to avoid overloading the filter. After filtration, particles deposited

on the surface filter were coated by a second carbon layer and transferred directly onto gold electron microscope grids by dissolving under suction the filter substrate with chloroform (Sebastien et al., 1978). Each grid (3 mm in diameter, 200 mesh of 6400 μm^2 each) was analysed using a JEOL 100 C Transmission Electron Microscope fitted with an EDAX 711 X-ray Energy Dispersive Spectrometer (XEDS) interfaced with a computer. For a single particle, this instrumentation simultaneously allows:

observation of particles as small as 0.1 micron;

determination of the crystalline structure using the electron diffraction pattern;

determination of the chemical composition, obtained by X-ray spectrometry.

Operating conditions for analysis were as follows: grid mounted in a carbon receptacle, 35° tilt angle in the direction of detector; accelerating voltage 100 kV; accumulation time 40 to 80 s; size of focused beam 0.3 micron.

In order to identify the mineral phases, an analytical strategy (summarized by Table 1) was developed using the three parameters to obtain

Table 1. *Strategy used for mineralogical identification of particles*

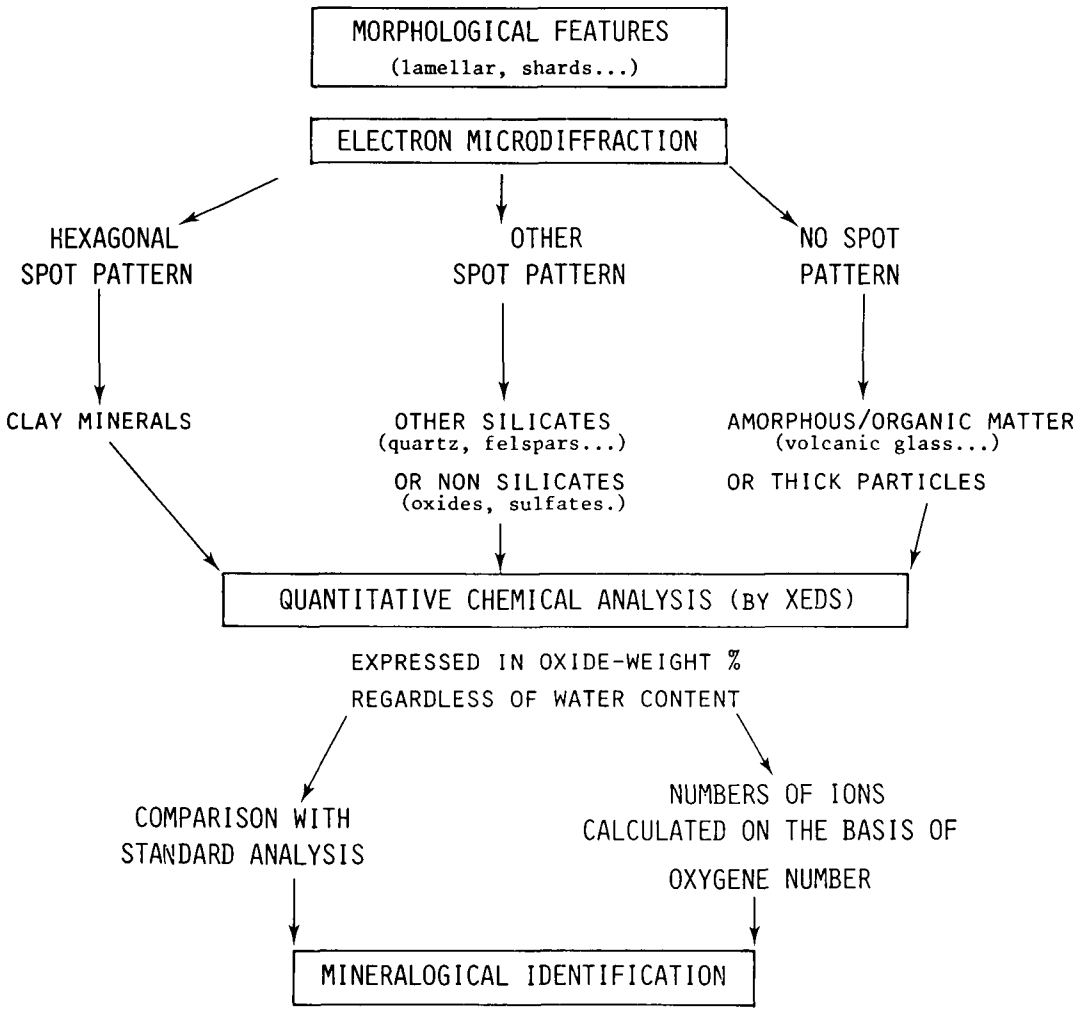

a step-by-step diagnosis (Gaudichet, 1984). Particles can be identified by:

(1) their morphology, including their shape (lamellar, fibrous, choncoïdal, shard);

(2) their electron diffraction pattern, observed directly under the microscope, allowing to distinguish between crystalline and amorphous particles, useful to characterize volcanic glasses, for example, and to quickly recognize from other silicates, such as silica and felspars, sheet silicates, such as clays, always flat laid on the filter according to their (001) plane and exhibiting a hexagonal electron diffraction pattern;

(3) their mineral species as given by their elemental chemical composition. The X-ray dispersive spectrometer allows a qualitative determination, for each particle, of elements present with an atomic number Z greater than 10. However, the identification of particles based only on qualitative chemical analysis is inaccurate because possible confusions can remain between minerals composed of the same elements such as muscovite [$KAl_2(Si_3AlO_{10})(OH)_2$] and potassium felspar [$K(Si_3AlO_8)$]. We therefore made a quantitative assessment of the elemental composition using the peak ratio method taking Si as a reference element, assuming that particles can be considered as thin (less than 2 μm) layers (Cliff and Lorimer, 1975). The spectrometer was calibrated by the analysis of standard minerals in order to determine the Cliff-Lorimer k factors at operating conditions for each element. Using this method, the elemental composition is known with an accuracy better than 3%.

Peak ratio data were computerized in order to express the chemical information in terms of oxide weight percentages, regardless of water content, to be compared with minerals described in existing literature (Deer et al., 1967).

In practice, quantitative microanalysis and microdiffraction allowed us to identify the majority of natural mineral particles, especially silicates. Moreover, it is possible to check the validity of such diagnoses, by comparing the structural formula calculated from the experimental chemical analysis and the theoretical formula for each mineral.

The frequencies of mineral species were obtained by scanning, at direct magnification ($\times$10,000 to $\times$33,000), randomly chosen mesh (6400 μm^2) in which each particle encountered was identified.

3. Results and discussion

A total of 225 particles were analysed for the six selected samples. Most of the particles were smaller than 2 μm. Grain size distribution of particles was not investigated here because of the insufficient number of observations. Mineralogical identification through the diagnosis scheme was possible on an average of 80% of the cases. Diagnosis was sometimes impossible for one of the following reasons:

(1) particles thicker than 0.2 μm are not permeable under electrons, then it is impossible to obtain electron diffraction pattern;

(2) particles overlapped, giving mixed silicate chemical compositions. Indeed the ATEM observation revealed that a significant number of observed particles were constituted by numerous aggregates (see Fig. 3), especially of fine clay minerals, and they may have been taken as isolated particles in previous Analytical Scanning Electron Microscopy (ASEM) studies (e.g. De Angelis et al., 1984);

(3) elemental composition could not be related to a known mineral in the literature.

The number and the relative abundance of minerals identified in the 6 samples are reported in Table 2. A statistical approach (binomial distribution) did not indicate a significant difference (95% of confidence level) in the relative abundance of mineral dusts from terrigenous origin (such as clays, and feldspars) from one level to another by comparison with the mean content of each species pooled from the six samples analysed. One sample corresponding to the LGM (552 m) has a quartz content significantly higher than the mean content. In one sample corresponding to the Holocene period at 245 m of depth, the presence of volcanic glass particles was significantly different from the other samples. Particle mineralogy is mostly represented by various silicate materials such as clay minerals (40%), quartz (Fig. 4) (13%) and felspar (18%). Volcanic glass shards (Fig. 4) (mainly at the 245 m level) as well as some ferruginous, titanium oxide (or hydroxide),

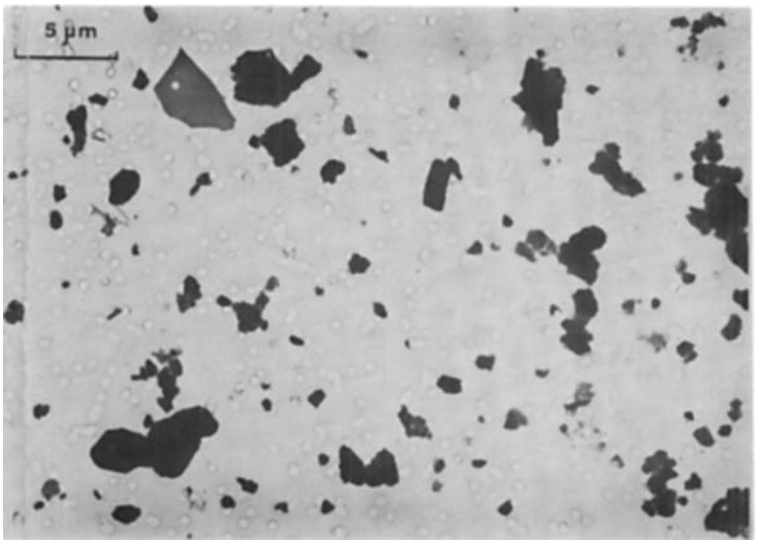

Fig. 3. TEM microphotographs at low magnification of the grid after dissolution of the filter. The prints of filter pores appear as round white areas, and particles (in black) are either well isolated or constituted by aggregates of fine minerals. Scale bar is 5 μm.

Table 2. *Number (n) and relative abundance (% in brackets) of minerals identified in each of the 6 sample levels, compared with the mean content of each mineral species (*statistically significant difference from the average at a 95% confidence level according to a binomial distribution)*

	246		345		552		580		678		838		Average	
Dome C sample depth (m)	*n*	(%)	*n*	(%)	*n*	(%)	*n*	(%)	*n*	(%)	*n*	(%)	*n*	(%)
—clays: Illite	9	(34)	16	(38)	10	(28)	13	(26)	7	(32)	17	(34)	12	(32)
kaolinite	1	(4)	1	(2)	1	(3)	—		—		—		0.5	(1.5)
chlorite	—		2	(5)	1	(3)	2	(4)	1	(5)	3	(6)	6	(5)
smectite	—		1	(2)	—		3	(6)	—		—		0.6	(1.3)
—crystalline silica	3	(12)	4	(10)	8*	(23)	6	(12)	3	(13)	4	(8)	5	(13)
—amorphous silica	—		1	(2)	2	(6)	2	(4)	—		—		0.8	(2)
—felspars	4	(15)	8	(19)	8	(23)	11	(22)	3	(13)	9	(18)	7	(18)
—pyroxenes-amphiboles	—		2	(5)	2	(6)	—		1	(5)	1	(2)	1	(3)
—metallic oxides	1	(4)	2	(5)	—		3	(6)	—		—		1	(2.5)
—volcanic glass	3*	(11)	—		—		—		1	(5)	—		0.6	(2.6)
Others (overlapped or unidentified)	5	(19)	5	(12)	3	(8)	10	(20)	6	(27)	16	(32)	7.5	(20)
Total number	26		42		35		50		22		50			

pyroxene and amphibole particles were detected, but in small proportions. A new observation for Antarctic ice is the presence of diatom fragments (Fig. 5), composed of amorphous silica and easily recognizable by their morphology. Diatom frustules have been also observed in Greenland ice (Gayley and Ram, 1984).

We will now focus the discussion on clay minerals, quartz, and felspar, which are the major components. We will also discuss the volcanic

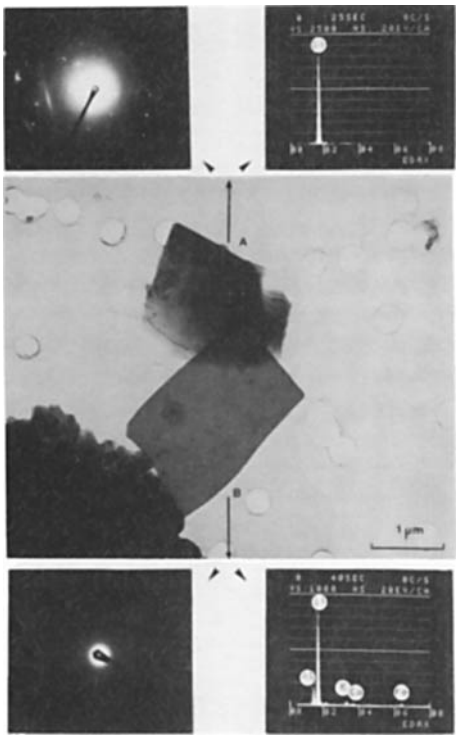

Fig. 4. TEM microphotograph with corresponding diffraction pattern and XEDS spectrum of two particles observed in the 246 m sample level. At the top, the quartz particle (A) is clearly distinguished by its electron diffraction pattern from the amorphous volcanic glass shard (B) at the bottom.

glasses because of their potential for souce identification in spite of their small proportions.

3.1. Clay minerals

Clay minerals were identified in 40% of total number of the particles, among this clay 32% of them may be classed in the illite group. No significant variation (binominal distribution with 95% confidence level) in the relative frequency was observed between the samples.

Illite is a world-wide detritic component of sediments. In the fraction smaller than 2 microns, it represents 30% of the mass of deep sea sediments (Griffin et al., 1968). It is present in the Sahara dust outbreaks (Glaccum and Prospero, 1980) as well as in dust plumes from the Asian continent (Gaudichet and Buat-Menard, 1982; Blank et al., 1985). For Antarctic aerosol, Kumai (1976) used the electron diffraction pattern in a TEM, and observed that 34% of the central nuclei of snow crystals collected at the geographic South Pole are illites. However, since his study covers only few days of aerosol collection, the fact that this illite content is close to our value might be fortuitous. In tropical Pacific air, dust collected on the Eniwetak Atoll showed strong seasonal variation of illites between 47% in April and 18% in July depending on the atmospheric circulation and dust source influences (Gaudichet and Buat-Menard, 1982; Buat-Menard et al.,

Fig. 5. TEM microphotograph and XEDS spectrum (silicon signal) of a diatom fragment.

1982). Our data does not suggest any variation of this type from level to level over the studied period. This could be due to the smoothing of the seasonal fluctuations, each sample including the precipitations of several years.

Three kaolinite clay minerals have been identified (Fig. 6), representing only 1.3% of the 225 particles analysed. This appears very low compared to the 10% found by Kumai (1976): the score was 7 kaolinite clays identified from 74 non sodium-chloride (i.e., non-soluble) particles. In fact, besides the possible influence of the different methods of sampling, for an hypothetical dust source with 4% of kaolinite content, Kumai's data as well as our data could be scored by a statistical approach (binomial distribution) as the high (Kumai's data) and low (ours) limits respectively of the 95% confidence interval. However, when our data are pooled, excluding the two Holocene samples, the data are out of the lower limit of this interval suggesting a source with very low (<4%) kaolinite content, especially during glacial climate.

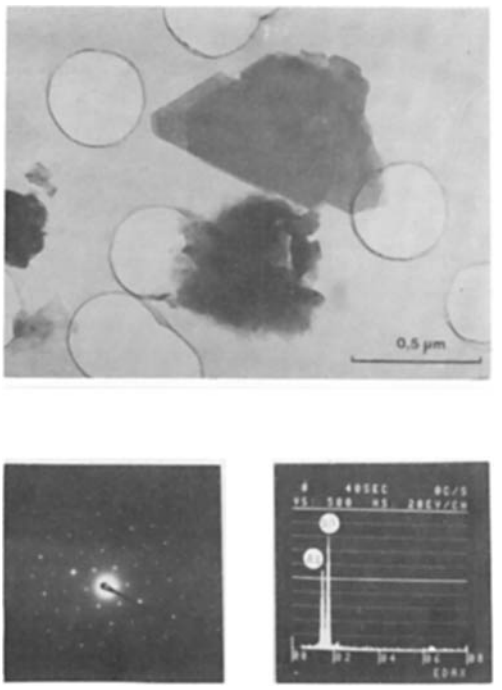

Fig. 6. TEM microphotograph with corresponding diffraction pattern and XEDS spectrum of a kaolinite clay. Note the typical morphology of this clay particle showing the superposition of sheets and the hexagonal electron diffraction pattern.

Kaolinite is considered to be a low latitude clay (Griffin et al., 1968) formed by an intense weathering process. On a world-wide scale, a high proportion (up to 90%) of this clay is found in a belt bounded by the tropics. For example, high concentrations were found in the smaller than 2 μm fraction of the Australian desert coupled with iron oxide, as well as in the aerosol dust from aeolian deflation (Prospero and Merrill, 1980) and in the surrounding deep sea sediments (Griffin et al., 1968). The low proportion of kaolinite found in our samples, integrating a 3 to 5 year period, suggests that Australian deserts and low latitude tropical areas are not the main direct sources of Dome C microparticles.

5% of the particles were identified as chlorite clays. As opposed to kaolinite, chlorite may be characterized as the "high latitude clay mineral found in abundance in polar regions of the world where chemical destruction is low" (Griffin et al., 1968). Therefore, if we eliminate the low latitude tropical area because of the low values of kaolinite, and the small area of exposed ground in Antarctica (i.e. dry valleys), then the tip of South America including the Patagonian area, appears to be a good candidate for Antarctic dust. By contrast with Australia, South of 40° latitude, the high mountains of the Andes Cordilliera are swept by continuous westerlies giving a semi-arid to arid desert climate on the East side of the Andes (Patagonia). The presence of glaciers induces cold and dry winds favourable to ground deflation, accumulation of periglacial and/or peridesertic loess and thence to the mobilization of dust (Charlesworth, 1957; Flint, 1971). Moreover, the environmental conditions propitious to dust production probably have been enhanced during LGM where South America was drier and more windy than at present (Damuth and Fairbridge, 1970; Heusser, 1981). During the LGM, the 120 m-lowering of the sea level (Climap, 1981) South of 40° latitude allowed the additional exposure of a 10^6 km^2 area of continental margins thus doubling the present emerged land area, and of unconsolidated material.

Small-sized dust injected at high altitude (e.g., above 3000 m a.s.l.) in the 40°S westerlies would

be transported southward over the Antarctic continent along with the penetration of depressions. We have no direct proof of production and long range transport of South American dust in the Southern Hemisphere but contribution of this continent to Antarctic aerosol is also suggested by detection of "radonic storms" (radon 222 is a short lived natural radionuclide originating from continental soils) suddenly arriving at various Antarctic locations (Lambert et al., 1970). Moreover, numerical simulations of continental dust spreading using an Atmospheric General Circulation Model (AGCM) (Joussaume, 1983, 1985; Joussaume et al., 1984) suggest, for present climatic conditions in a 30 days simulation, South America and Australia as main sources of dust for Antarctica. However, according to these simulations the American source would be dominant for Central Antarctica (i.e. near the geographic South Pole) while Australia would dominate in East Antarctica (as Dome C site). These results do not exactly match our above suggestions; discrepancy may be due to the use of a low-resolution AGMC or/and the short time duration of the simulation. For the future, search for kaolinite clay in snow in other Antarctica locations should be very useful as a check for simulations using a higher resolution AGCM and performed under both present and LGM climatic conditions.

3.2. *Crystalline silica minerals*

Crystalline silica (quartz or tridymite) represents 13% of the identified particles. Except for the 552 m sample, the quartz proportion remains constant from sample to sample.

Quartz is a terrigenous mineral, one of the most resistant to weathering agents. It is present in many sediments and aerosols and by contrast with the other minerals, is rather well identifiable under ASEM (Petit et al., 1983) but may be confused with other allotropic forms of silica (such as opal of the diatoms). Quartz abundance has been used as continental aridity index in continental and deep sea sediment records (Bowles, 1975; Molina-Cruz, 1977; Bowler, 1976; Venkatarathan and Biscaye, 1977; ...). Using similar approach for Dome C and Vostok ice records, ASEM previous studies (Briat et al., 1982; Petit et al., 1983) have shown higher abundance of quartz particles in samples from LGM climate as well as the presence of quartz particles larger than 5 μm. This was interpreted as the print of the LGM environment characterized by greater aridity and more efficient atmospheric circulation. The present study indicates similar results, but only for the 552 m sample in the LGM period. Moreover quartz and felspar particles have a similar shape (more or less spherical) and are therefore less fitted to suspension in wind than the plate like clays. From our data we get a higher value of the silica plus felspars to clay ratio for LGM samples than for other periods. This tends to support the idea of more efficient atmospheric circulation.

3.3. *Felspar composition*

Felspar represented 18% of all mineral particles and their compositions were plotted on a ternary diagram in terms of the three mineral species: albite, anorthite and orthoclase (Fig. 7). All types were encountered in each sample. Moreover, species such as calcic plagioclases, and potassic felspar which cannot come from the same rock, were observed in the same ice sample. This suggests either that the air mass origin area can be mineralogically heterogenous, or that the mixing of particles coming from different areas takes place during their transport to Antarctica. Another possibility is that our filtration process combines deposits corresponding to various

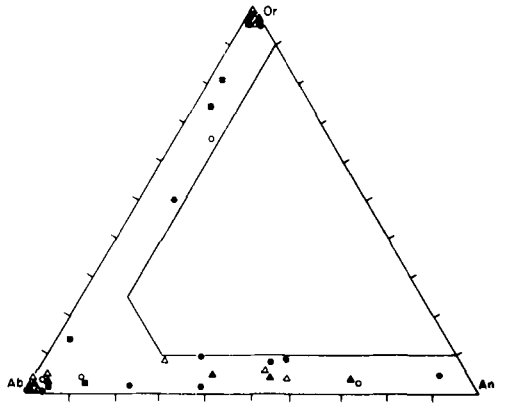

Fig. 7. Compositions of felspar reported on a triangle diagram orthoclase (Or)—albite (Ab)—anorthite (An) corresponding to the studied Dome C samples: solid dot (580 m) open dot (346 m), solid triangle (552 m) open triangle (678 m), solid square (838 m).

sources since our ice samples cover 2 to 5 years of accumulation.

3.4. Volcanic glass composition

Volcanic glass shards were looked for at a low magnification ($\times 5000$ to 10,000) on grids in all our samples, in addition to the study of all particles on a randomly chosen area of the filter, due to their potential use as an indicator of their sources. Glass shards were found in three samples and the frequency is the highest at level 246 m suggesting a volcanic activity print. This was independently confirmed by a study on aliquots of this sample made by Fehrenbach (1984) using an ASEM. In addition, we observed some clays and silica at this level showing unusual sulfur signals on XEDS spectra (Fig. 8). This could be the result of the adsorption of sulfur, produced by volcanoes, on atmospheric particles of terrigenous origin, during air mass transport through volcanic plumes (Smith and Zielinski, 1982).

In spite of the instability of glass particles under the electron beam, resulting especially in loss of sodium content, their quantitative chemical analysis is reported in Table 3. They are probably depleted in sodium content giving a relative increase in the percentage weight of the other elements. Taking into account this problem, our mean analysis of the 6 volcanic glasses from 246 m level is in good agreement with the mean composition obtained by Fehrenbach (1984) from the analysis of 20 particles coming from 27 of the same samples and can be related to a ryolitic composition. Moreover, we observed that some crystalline silica at this level showed shard morphology, that could be related to a volcanic activity of hypersiliceous magmas. Five other volcanic glasses analysed by Fehrenbach were quite different and were related to a trachytic composition, whereas 2 other glasses were dacitic in composition.

The scanning of the grid corresponding to level 838 m revealed two volcanic glass particles, chemically similar to the glass shards from the Byrd ice core and the volcanic particles from the 726 m Dome C ice sample analysed both by Kyle et al. (1981). These glass shards, composed of peralkaline trachyte could be the result of localized Antarctic volcanic activity.

Finally 5 volcanic glasses were encountered in the 678 m ice sample. Two of them were ryolitic and three had an unusually low (2.5%) alumina content and a very high (82%) silica content. Globally, except for one Holocene ice sample (278 m), volcanic glass remains a very minor atmospheric contaminant, before and during the corresponding LGM sample period. Moreover, their compositions are variable from one level to another and also within one level, suggesting numerous origins.

4. Conclusion and future work

This study offers additional evidence of an aeolian terrigenous origin for the main portion of insoluble microparticles at Dome C over the last

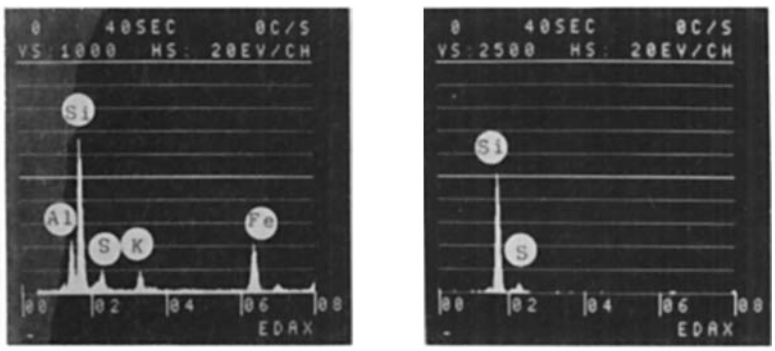

Fig. 8. XEDS spectra of an illite particle and a quartz particle containing an unusual sulfur component (sample 246 m).

Table 3. *Elemental composition (% oxide) of volcanic glass shards from Dome C and Byrd ice cores. Samples are 246 m, 678 m, 838 m from this study; F 246 data is from 246 m studied by Fehrenbach (1984); Dome C 726 m and Byrd samples are from Kyle et al. (1981). *Fe T represents Fe_2O_3 + FeO content and n the number of analyzed glass shards*

Sample references	Na_2O	MgO	Al_2O	SiO_2	K_2O	CaO	TiO	MnO	FeT
246 m $n = 6$	0.1	0.1	14.3	77.9	2.3	2	0.4	0	2.5
F 246 $n = 20$	2.9	0.5	15.4	74.6	2.7	1.3	0.4	0	2.2
678 m $n = 2$ $n = 3$	0 0	0 1.9	14.7 2.5	76 82.2	5.5 1.4	1.5 9	0.3 1	0 0	1.8 2.2
838 m $n = 2$	2.2	0	16	63.4	6.9	1.8	0.9	0.4	7.9
Dome C 726 m $n = 16$	6.6	0.1	14.1	61.7	4.4	1.2	0.5	0	8.8
Byrd $n = 101$	7.8	0.1	15.1	61.9	4.5	1.6	0.5	0	7.9

30,000 years. Moreover, in spite of the low number of analyzed particles, this study pointed out that mineral species observed in all samples seem to remain almost the same proportion from one sample to another. Thus, the increase of the total amount of particles during the LGM concerns most of terrigenous particles species and confirms previous conclusions (Petit et al., 1981; Briat et al., 1982): larger extension of ariditic zones and accelerating of atmospheric processes during the LGM.

Volcanic glasses obviously in small proportion are rather abundant in one Holocene sample, whereas scarce before and during the LGM samples. Their compositions are varied and suggest multiple possible sources, either local or distant.

Clay minerals are clearly identified for the first time in this core. Kaolinite clay was observed only in the 246 m, 345 m, 552 m ice samples. The low proportion of kaolinite found gives less support to low latitude tropical areas of the Southern Hemisphere as major sources of Dome C dust. South America, with Patagonia and Andes Cordillera now appears a better candidate. This hypotheses needs to be confirmed by studying more particles from other samples of Dome C and from other Antarctic ice cores, as well as by mineralogical studies of aerosols produced by South America.

Finally this information may be useful in a first step for checking for present and past climate numerical simulations of atmospheric circulation and dust sources and transport. These studies would help in evaluating the impact of dust on past climatic changes.

5. Acknowledgements

This work was supported in the field by Terres Australes et Antarctiques Françaises, Expéditions Polaires Françaises and the National Science Foundation (Division of Polar Programs).

REFERENCES

Bigg, E. K. 1980. Comparison of aerosol at four baseline atmospheric monitoring stations. *J. Appl. Meteorol. 19*, 521–580.

Blank, M., Leinen, M. and Prospero, J. M. 1985. Major asian aeolian inputs indicated by the mineralogy of aerosols and sediments in the Western North Pacific. *Nature 314*, 84–86.

Bowler, J. M. 1976. Aridity in Australia, origin and expression in aeolian landforms and sediments. *Earth Sci. Rev. 12*, 279–310.

Bowles, F. A. 1975. Paleoclimatic significance of quartz/illite variations in core from the Eastern equatorial North Atlantic. *Quaternary Res. 5*, 225–235.

Briat, M., Royer, A., Petit, J. R. and Lorius, C. 1982. Late glacial input of eolian continental dust in the Dome C ice core: additional evidence from individual microparticles analysis. *Ann. Glaciol. 3*, 27–31.

Buat-Ménard, P., Ezat, U. and Gaudichet, A. 1982. Size distribution and mineralogy of alumino-silicate dust particles in tropical pacific air and rain. In *4th International Conf. on Precipitations Scavenging Dry depositon and Resuspension* (ed. Pruppacher et al.). Elsevier Science Publishing, 1259–1269.

Charlesworth, J. K. 1957. *The Quaternary era* (Arnold Pub., London), 2 Vol., 1700 p.

Cliff, G. and Lorimer, G. W. 1975. The quantitative analysis of thin specimens. *J. Microsc. 103*, 203–207.

Climap Project Members 1976. The surface of the Ice-Age. Earth. *Science 191*, 4232, 1131–1137.

Climap Project Members 1981. Seasonal reconstructions of the Earth's surface at the last Glacial Maximum. *The Geological Society of America*, Map and Chart series, MC 36.

Cragin, J. H., Herron, M. M., Langway, C. C. Jr, and Klouda, G. 1977. Interhemispheric comparison in changes in the composition of atmospheric precipitation during the last Cenozoïc era. In *Polar Oceans* (ed. M. J. Dunbar). Arctic Institute of North America, Calgary, 617–631.

Cunningham, W. C. and Zoller, W. H. 1981. The chemical composition of remote area aerosol. *J. Atmos. Sci. 12*, 367–384.

Damuth, J. E. and Fairbridge, 1970. Equatorial Atlantic deep-sea arkosic sands and Ice Age aridity in tropical South America. *Geol. Soc. Amer. Bull. 81*, 189–206.

Dansgaard, W., Johnsen, S. J., Clausen, H. B. and Langway, C. C. Jr. 1971. Climatic record revealed by Camp Century ice core. In *The Late Cenozoïc Glacial Ages* (ed. K. K. Turekian). New Haven Conn.: Yale University Press, 37–56.

De Angelis, M., Legrand, M., Petit, J. R., Barkov, N. I., Korotkevich, Ye. S. and Kotlyakov, V. M. 1984. Soluble and insoluble impurities along the 950 m deep Vostok ice core (Antarctica). Climatic implications. *J. Atmos. Chem. 1*, 215–239.

Deer, W. A., Howie, R. A. and Zussman, J. 1967. *Rock-forming minerals*. London: Longsman Publ., Vol. 1 to 5.

Fehrenbach, L. 1984. Analytical microscopy of volcanic glass microparticle fall out in polar ices (Microscopie analytique de micro-particules de verre volcanique piégées dans les glaces polaires). *Bulletin PIRPSEV-CNRS 94*, 85 p.

Fisher, D. A. 1979. Comparison of 10^5 years of oxygen isotope and insoluble impurity profiles from the Devon Island and Camp Century ice cores. *Quaternary Res. 11*, 299–305.

Flint, R. F. 1971. *Glacial and quaternary geology* (John Wiley et Sons, Inc.), 892 p.

Gaudichet, A. 1984. Characterization of fine particles in atmospheric samples by analytical transmission electron microscope. *J. Phys. 45*, $C_2$789 $C_2$792.

Gaudichet, A. et Buat-Ménard, P. 1982. Mineralogy and origin of atmospheric particles over the Tropical North Pacific (Enewetak Atoll) by analytical transmission electron microscopy. (Nature minéralogique des particules insolubles du Pacifique Tropical Nord (Atoll d'Eniwetak) Etude par microscopie électronique analytique en transmission.) *C. R. Acad. Sci. Paris 294*, 1241 1246.

Gayley, R. I. and Ram, M. 1984. Observation of diatoms in Greenland ice. *Arctic 37*, 2, 172–173.

Glaccum, R. A. and Prospero, J. M. 1980. Saharan aerosols over tropical North-Atlantic Mineralogy. *Mar. Geol. 37*, 295–321.

Gow, A. J. and Williamson, T. 1971. Volcanic ash in the Antarctic sheet and its possible climatic implications. *Earth Planet. Sci. Lett. 13*, 210 218.

Griffin, R. J., Windom, H. and Goldberg, E. D. 1968. The distribution of clay minerals in the world ocean. *Deep-Sea Res. 15*, 433–459.

Heusser, C. J. 1981. Palynology of the last interglacial-glacial cycle in midlatitudes of Chile. *Quaternary Res. 16*, 293 321.

Joussaume, S. 1983. Simulation of water isotopes and desert-dust aerosol in an atmospheric general circulation model. (Modélisation des espèces isotopiques de l'eau et des aérosols d'origine désertique dans un modèle de circulation générale de l'atmosphère.) *Thèse de 3ème cycle*, Université Pierre et Marie Curie, Paris, 226 p.

Joussaume, S., Rasool, I., Sadourny, R. and Petit, J. R. 1984. Simulation of dust cycles in an atmospheric general circulation model. *Ann. Glaciol. 5*, 204–207.

Joussaume, S. 1985. Simulation of airborne impurity cycles using atmospheric general circulation models. *Ann. Glaciol. 7*, 131 137.

Kyle, P. R., Jezek, P. A., Mosley-Thompson, E. and Thompson, L. D. 1981. Tephra layers in the Byrd

Station ice core and the Dome C ice core, Antarctica and their climatic importance. *J. Volc. Geotherm. Res. 11*, 29–39.

Kumai, M. 1976. Identification of nuclei and concentrations of chemical species in snow crystals sampled at the South-Pole. *J. Atmos. Sci. 33*, 833–841.

Lambert, G., Polian, G. and Taupin, D. 1970. Existence of periodicity in radon concentrations and in the large scale accumulation at lower altitude between 40° and 70° South. *J. Geophys. Res. 75*, 2341–2345.

Lorius, C., Merlivat, L., Jouzel, J. and Pourchet, M. 1979. A 30,000 yr isotopic climatic record from Antarctic ice. *Nature 280*, 644–648.

Lorius, C., Raynaud, D., Petit, J. R., Jouzel, J. and Merlivat, L. 1984. Late glacial maximum Holocene atmospheric and ice thickness changes from Antarctic ice core studies. *Ann. Glaciol. 5*, 88–94.

Molina-Cruz, A. 1977. The relation of Southern trade winds to upwelling process during the last 75,000 years. *Quaternary Res. 8*, 324–338.

Petit, J. R., Briat, M. and Royer, A. 1981. Ice age aerosol content from East Antarctica ice core samples and past wind strength. *Nature 293*, 391–393.

Petit, J. R., Ezat, U., Barkov, N. I. and Petrov, V. N. 1983. Identification of quartz microparticles in 20,000 BP ice samples: a signature of the Last Glacial environment. *Scanning Electron Microscopy IV*, SEM inc., AMF O'Hare Chicago, 1627–1633.

Pourchet, M., Pinglot, F. and Lorius, C. 1983. Some meteorological applications from radioactive fall out measurements in Antarctic snow. *J. Geophys. Res. 88*, C10, 6013–6020.

Prospero, J. and Merrill, J. 1980. Preliminary report. *Searex Newslett. 3*, 3, 30–31.

Sarnthein, M. 1978. Sand deserts during glacial maximum and climatic optimum. *Nature 272*, 43–46.

Sebastien, P., Billon-Galland, M. A., Janson, X., Bonnaud, G. and Bignon, J. 1978. The use of transmission electron microscopy (TEM) for study of albestros contamination. (Utilisation du microscope électronique à transmission (MET) pour la mesure des contaminations par l'amiante.) *Arch. Mal. Prof. 39*, 229–248.

Shaw, G. E. 1980. Optical and physical properties of aerosols over the Antarctic ice sheet. *Atmos. Environ. 14*, 911–921.

Smith, D. B. and Zielinski, R. A. 1982. Water soluble material on aerosols collected within volcanic eruption clouds. *J. Geophys. Res. 87*, 4963–4972.

Thompson, L. G. 1977. Microparticles, ice sheets and climate. *Institute of Polar studies report 64*, 147 p.

Thompson, L. G. and Mosley-Thompson, E. 1981. Microparticle concentration variations linked with climatic change: evidence from polar ice cores. *Science 212*, 812–814.

Venkatarathnan, K. and Biscaye, P. 1977. Distribution and origin of quartz in the sediments of the Indian Ocean. *J. Sediment. Petrol. 47*, 2, 642–649.

Wolff, E. W. and Peel, D. A. 1985. The record of global pollution in polar snow and ice. *Nature 313*, 535–540.